Available online at www.sciencedirect.com
SCIENCE @ DIRECT®

Polymer 45 (2004) 1167–1175

polymer

www.elsevier.com/locate/polymer

Use of the dielectric analysis to complement previous thermoanalytical studies on the system diglycidyl ether of bisphenol A/1,2 diamine cyclohexane

Lisardo Núñez*, S. Gómez-Barreiro, C.A. Gracia-Fernández, M.R. Núñez

Research Group TERBIPROMAT, Departamento Física Aplicada, Universidade de Santiago 15782, Santiago, Spain

Received 13 May 2003; received in revised form 6 October 2003; accepted 2 December 2003

Abstract

The dielectric analysis technique was used to characterize an epoxy cured system consisting of a diglycidyl ether of bisphenol A (DGEBA, $n = 0$) and 1,2 diaminecyclohexane (DCH). With this purpose, the permittivity ε', the loss factor ε'', and the dissipation factor tan δ were determined experimentally. The transition observed within the temperature range studied was associated to a α-relaxation process, the T_g of which was taken as that corresponding to the maximum of the $\varepsilon'' - T$ curve recorded.

Argand diagrams for the different temperatures were constructed, and owing to the asymmetry showed by these diagrams, the Havriliak–Negami model was used to analyze data. It was observed that, within the frequency range (0.1–300 Hz) used for this study, the relaxation time follows an Arrhenius behaviour, thus allowing calculation of the activation energy E_a and T_g in good agreement with literature values.
© 2003 Elsevier Ltd. All rights reserved.

Keywords: Dielectric analysis; Cured epoxy-diamine; Thermal analysis

---

1. Introduction

There are few synthetic organic materials offering as many applications as epoxy resins. Their use as adhesives for most substrates, protective coatings, body shoulders and caulking compounds, textiles, fibre reinforce plastics, varnishes, etc. make epoxy materials to be in great demand.

The highly polar nature of the specific epoxy group make epoxy resin derived materials very valuable to be studied by dielectric analysis (DEA). In this article, DEA was used to obtain data that joined to those previously achieved [1–5] in our laboratories through different thermal analysis techniques (DMA, TGA-FTIR, DSC, etc.) allow to increase the information about the physico-chemical properties of the DGEBA ($n = 0$)/1, 2 DCH epoxy system. Our objective is to complement previous studies on this system using the dielectric analysis technique. This selection was based on the fact that dielectric measurements are extremely sensitive to small changes in material properties mainly at molecular level, and, especially in its ability to detect the glass transition. Moreover, the theory of dielectric analysis was widely developed in the last decades. This work pretends to be the first of a series in which different aspects and properties of the epoxy system here studied and some other epoxy resin materials will be considered.

Dielectric analysis (DEA) measures changes in the properties of a material as a response to the application on it of a time dependent electric field. This technique is a perfect complement to the other different techniques of thermal analysis [6] by identifying the transitions from the electrical properties of the materials.

An advantage of DEA over other techniques, is the possibility of using a wider frequency range. Moreover, dielectric measurements are extremely sensitive to small changes in material properties (molecular relaxation of the order of only a few nanometer involves dipole changes that can be observed by DEA). This enables detection of transitions that would not be possible through other techniques. Particularly, DEA complements DMA for characterization of the internal motions in polymers [7]. Both techniques can detect many viscoelastic relaxations with the same relationship between frequency and temperature. However, DEA tends to be more sensitive to local

---

* Corresponding author. Tel./fax: +34-981524350.
E-mail address: falisar1@usc.es (L. Núñez).

0032-3861/$ - see front matter © 2003 Elsevier Ltd. All rights reserved.
doi:10.1016/j.polymer.2003.12.024

motions that involve the reorientation of dipoles in a material as it is subjected to an oscillating electric field.

For interpretation of dielectric measurements, it is assumed that the sample behaviour can be represented by a time-invariant linear admittance. In this case, linearity involves a proportional relationship between the applied voltage and the resulting current. The linearity of a given sample, depends on the magnitude of the applied voltage, and all dielectric experiences breakdown at electric fields of the order of 10^6 V cm^{-1}. Coln [8] has found no significant non-linear effects in liquid epoxy resins prior to cure (where ion conduction is most important) under normal measurements conditions, that is, voltages of the order of a few volts, with electrode spacing ranging from tens of micrometer to several millimeter.

The complex dielectric constant of a material can be separated into its real and imaginary parts where ε' is the relative permittivity (real part) and ε'' is the relative loss factor (imaginary part). Both are related to ε_0 the permittivity of the free space (equal to 8.85×10^{-12} F m^{-1}):

$$\varepsilon^* = \varepsilon' - \mathrm{i}\varepsilon'' \tag{1}$$

Both ε' and ε'' are functions of the measurement frequency. The ratio $\varepsilon''/\varepsilon'$ is known as the dissipation or loss tangent:

$$\tan\delta = \varepsilon''/\varepsilon' \tag{2}$$

where δ is the phase angle between the applied voltage and the current response.

As it was previously mentioned [8–12], when a sample is subjected to an applied electric field the dipoles in the material will orient in the direction of the electric field. The orientation process requires a characteristic time, called the *dipole relaxation time* and denoted by τ_d.

The simplest model to describe the orientation mechanism was developed by Debye [13] assuming a single relaxation time τ_d for all molecules. The resulting Debye expression for the relative permittivity and loss factor are:

$$\varepsilon' = \varepsilon_\mathrm{u} + \frac{(\varepsilon_\mathrm{r} - \varepsilon_\mathrm{u})}{1 + (\omega\tau_\mathrm{d})^2} \tag{3}$$

$$\varepsilon'' = \frac{(\varepsilon_\mathrm{r} - \varepsilon_\mathrm{u})\omega\tau_\mathrm{d}}{1 + (\omega\tau_\mathrm{d})^2} \tag{4}$$

to account for conductivity, can be written as:

$$\varepsilon'' = \frac{(\varepsilon_\mathrm{r} - \varepsilon_\mathrm{u})\omega\tau_\mathrm{d}}{1 + (\omega\tau_\mathrm{d})^2} + \frac{\sigma}{\omega\varepsilon_0}$$

where: ε_u = unrelaxed permittivity. ε_r = relaxed permittivity. τ_d = dipole relaxation time. σ = ionic conductivity. ε' has low values for polymers when measurements are performed at low temperature, that is, below thermal transitions because molecules are immobilised at their positions and the dipoles cannot move to orient in the direction of the electric field. This is also the reason why ε' is low in extremely crosslinked resins.

The relative loss factor, ε'', is a measure of the energy required for molecular motion, that is the energy dissipated in this motion in the presence of an electric field. It consists of two contributions: energy losses due to the orientation of molecular dipoles, and energy losses due to the conduction of ionic species. This last, begins to be significant at temperatures above the T_g value measured by DSC for this epoxy system.

A well recommended method to show the frequency dependence of ε' and ε'' is the Argand [10] Diagram, where ε'' is plotted vs. ε' taking ω as a parameter.

When the ionic conductivity, σ, is zero, the Argand diagram corresponding to Debye's model is a perfect semicircle with intercepts ε_u and ε_r at X-axis and with a maximum value of $(\varepsilon_\mathrm{u} - \varepsilon_\mathrm{r})/2$. As σ increases, the Argand diagram turns into a vertical line with an intercept ε_u at the ε' axis.

Practically, the observed Argand diagrams differ the ideal ones, due to various reasons, among them: ionic conductivity, electrode polarization, the existence of more than one dipole relaxation time for most part of materials, thus originating a distribution of relaxation times, causing some differences between calculated and observed results. Several empirical corrections modify the Debye model, among these, those proposed by Cole–Cole [14], Dadvison–Cole [15] and Havriliak–Negami [16–17].

This last will be used to analyse data presented in this article. According to it

$$\varepsilon^* = \varepsilon_\mathrm{r} + \frac{\varepsilon_\mathrm{u} - \varepsilon_\mathrm{r}}{(1 + (\mathrm{i}w\tau_\mathrm{d})^{1-a})^b} \tag{5}$$

where a and b are parameters $(0 < a < 1,\ 0 < b < 1)$ describing the symmetric and asymmetric broadening of the relaxation time distribution.

2. Experimental section

2.1. Dielectric analysis

Dielectric measurements were carried out using a dielectric analyser (DEA) 2970 from TA Instruments. The measurements assembly was the parallel plate structure.

The sensors must be calibrated for every experiment. These sensors use a geometrical value derived from the response of the electrode plate surface in mm^2, and value RTD corresponding to the resistance at 0 °C observed by the platinum thermometer in the base sensor.

The sample was under a maximum strength of 250 N, to ensure a good contact between the sample and the electrodes below T_g, and the heating rate was 2 °C/min. The minimum space between the top and the bottom electrodes was, according to the manual book and the maximum force, 0.501 mm, to prevent soft samples from being squeezed out of the sensor area during an experiment. All the experiments were carried out under a dry nitrogen atmosphere at a gas flow rate of 0.5 ml min^{-1}.

The experiments were carried out at fixed frequency values of 0.1, 0.2, 0.3, 0.5, 1, 3, 5, 10, 15, 20, 25, 40, 60, 80, 100, 125, 150, 175 and 200 Hz. The curve corresponding to de 200 Hz was not represented, as it does not give further information and make difficult the seeing.

2.2. Materials

Epoxy resin was diglycidyl ether of bisphenol A (DGEBA $n = 0$) (Resin 332, Sigma Chemical Co., St. Louis, MO) with an epoxy equivalent between 172 and 176 Curing agent was 1,2-diaminocyclohexane (DCH) (Fluka, Switzerland) 98% pure with an amine hydrogen equivalent weight of 28.5 and viscosity around 900 mPa s at room temperature.

Resin and diamine were carefully and homogeneously mixed at stoichiometry ratio 100:16.42. Once mixed, the sample was introduced into a frame to cure. The frame consists of two steel plates covered by two smooth teflon sheets and a teflon pattern with 20 holes of 2.5 × 2.5 cm and 0.5 cm thick.

Curing of the systems was achieved according to a TTT diagram previously designed [18] for this epoxy system consisting of two steps: a first one of 24 h at room temperature followed by a second one 16 h at 70 °C.

3. Results and discussion

Dielectric characterization of the system DGEBA ($n = 0$)/1, 2 DCH was made through isochrone and isothermal measurements. In the first mode, the temperature response of the material at different frequencies was measured, and the glass transition temperature T_g, was obtained from these measurements as that corresponding to the maximum of the ε'' (loss factor) vs. temperature plot. Second type of measurements was made at constant temperature and different frequencies. These last measurements are very useful [19] to analyse the dielectric behaviour of a material through the Argand diagram and the equation developed by Havriliak–Negami (H–N).

Dielectric permittivity is related to the capacitive nature of a material, that is, to its ability to store energy. Permittivity is a measure of the polarization of the medium per applied electric field [9]. Most organic resins have permittivities ranging from 2 to 10. As shown in Fig. 1, the system DGEBA ($n = 0$)/1, 2 DCH follows this trend for all the frequencies used in this study.

As a material, such as an epoxy resin, is heated through its α-transition temperature, dipoles gain enough energy and so enough mobility to orient in the electric field. This relaxation process generally causes an increase in permittivity with a corresponding loss factor peak. This effect is related to a dipole transition and has a characteristic relaxation time associated [20].

Fig. 1 is a plot of the real part, ε', of the complex permittivity against temperature. In it, a typical behaviour of a cured thermoset as a function of temperature and frequency can be observed. For the epoxy system here studied, the contribution of dipoles to permittivity, at low frequencies, begins in the temperature range between 135 and 150 °C in which the T_g value determined by DSC is included [18].

For construction of Argand diagrams and to fit data to the Havriliak–Negami equation, temperatures slightly above this temperature range were selected. By this selection, we ensured the coherence between the dielectric response and the objectives of our study.

At low frequencies, it can be observed a dramatic increase in ε' from 230 °C on. This effect is due to the substantial electrode polarization [21] occurring at this temperature.

The loss factor ε'' is related to the conductive nature of a material. The dielectric loss factor originates from two sources: energy loss associated with the time dependent polarization, and bulk conduction mainly due to impurities in the material. At temperatures well below T_g, polymers generally have loss factors less than 0.1. When heated to T_g, and above, they can have loss factors [9] as high as 10^9.

Ionic conduction is the result of current flow due to the motion of mobile ions within the material under test. It has been shown that concentrations well below 1 ppm are enough to originate significant ionic conduction levels (Senturia and Sheppard [12]). From the Debye [13] model, it is seen that ionic conduction contributes only to the loss factor and does not influence on the permittivity as long as electrode polarization is insignificant (see Eqs. (3) and (4)).

Fig. 2 shows the temperature dependence of the loss factor at different frequencies. The glass transition temperature, T_g, can be determined as that corresponding to the maximum in a $\varepsilon'' - T$ curve at every frequency. As it can be seen, below the glass transition temperature, the loss factor takes values less than 0.1, about 0.05, as expected.

It can also be observed, that from 205 °C approximately, ε'' undergoes a dramatic increase as a consequence of an increase in ionic conductivity. This causes, as it was previously mentioned, electrode polarization. Because of this, temperatures lower than 195 °C were considered for data analysis, thus giving a margin of error of 10 °C.

For this study, a temperature range from 160 to 195 °C was chosen thus to ensure the dipole relaxation as the only contribution to ε^*.

The distribution of ε'' curves follows the usual trend.

It must also be pointed out that the frequency range is limited since above 300 °C the sample begins to degrade, thus hindering the visualisation of the ε'' maximum.

Fig. 3 is a plot of tan δ vs. T at various frequencies. As it can be seen, tan δ behaves in a very similar way to that shown by ε'' with maximum following the same trend.

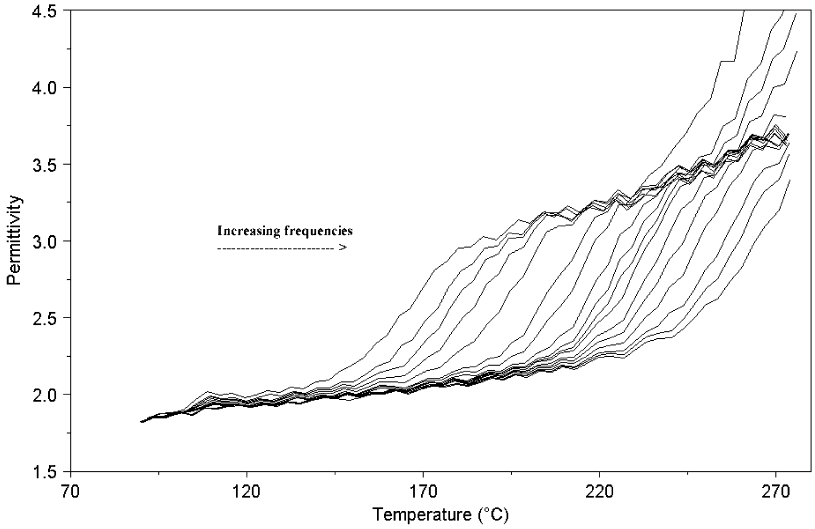

Fig. 1. Plot of permittivity versus temperature for the epoxy system DGEBA ($n = 0$)/1, 2 DCH in the range from 80 to 280 °C at the various frequencies (see text) used in this study.

Plots of ε' and ε'' against $\ln f$ at the different temperatures used for our isothermal experiments are presented in Fig. 4a and b, respectively. From these curves an Argand diagram, $\varepsilon' - \varepsilon''$, was constructed in the temperature range 160–195 °C (see Fig. 4c). Data in Fig. 4a and b, corresponding to the real and imaginary parts of the complex relative permittivity, respectively, were fit to Eq. (5) to obtain values [22] for the parameters a, b, τ, ε_r, ε_u and σ. These values are recorded in Table 1. The ionic conductivity, σ, was calculated from the frequency-independent portion of the loss factor data, that is, where a log–log plot of loss factor versus frequency has a slope of -1, using [9] the relationship $\varepsilon'' = \sigma/\omega\varepsilon_0$. The analysis of Figs. 1 and 2 demonstrated that ionic conductivity is not important within the temperature range used for this study. However, this term was included to separate the dipole and conductive parts in the loss factor.

A plot of σ vs. T shows a constant value of $9 \times 10^{-15}\ (\Omega\ \mathrm{cm})^{-1}$ for σ, much lower than those able to influence on losses. This result confirms our work hypothesis. To characterize the α-transition both from ε' and ε'', through H–N equation we pretend that only dipole contribution to the loss factor avoiding ionic contribution. By the choice of this constant value, we ensure a non-significant contribution of conduction to the loss factor, and also that within the temperature range studied, the conductivity do not increase with T and thus without contributing to the loss factor.

Plots of the above mentioned parameters versus temperature are shown in Fig. 5(a)–(e). In this figure, it can be observed that the parameter a, related to the relaxation times distribution width, increases linearly with temperature from a value close to zero. To improve information about dielectric behaviour, temperatures slightly below 140 °C

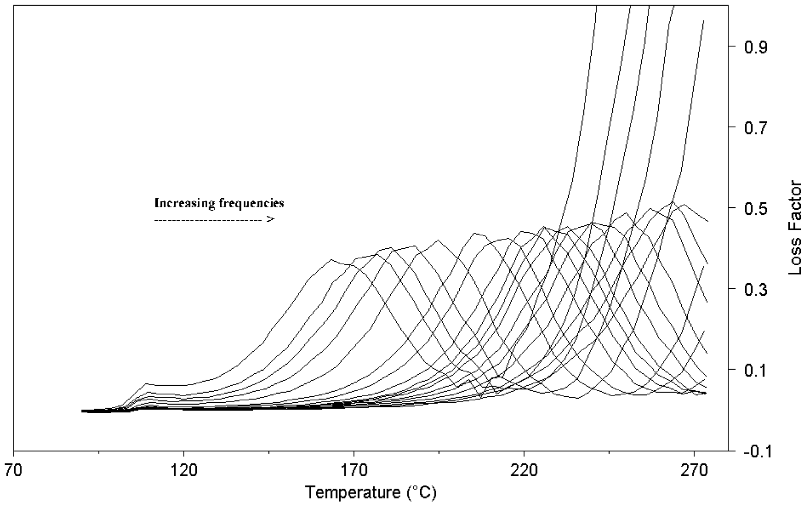

Fig. 2. Plot of loss factor versus temperature for the epoxy system DGEBA ($n = 0$) in the range 80–280 °C at the various frequencies (see text) used in this study.

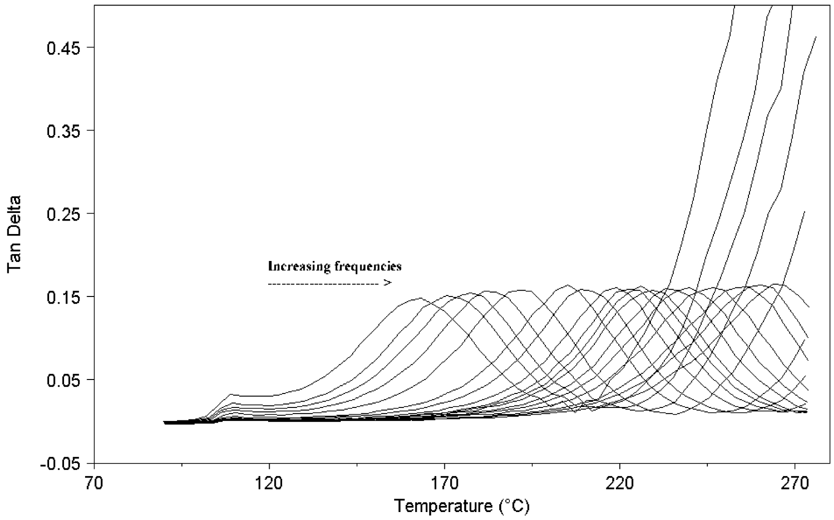

Fig. 3. Plot of tan δ versus temperature for the epoxy system DGEBA ($n = 0$)/1, 2 DCH in the range from 80 to 280 °C at various frequencies.

were chosen to study again ε' and ε'' as functions of temperature using Havriliak–Negami equation. We made calculations at temperatures below 160 °C, in order to have an idea of how the parameter a changes at values close to the α-relaxation. It was found that the error when fitting experimental data through H–N equation is same order at temperatures above or below 160 °C. It was observed that the parameter a remains constant at a value of zero up to a temperature of 160 °C. At this temperature dipoles with different relaxation times begin to contribute to relaxation thus originating widening around the characteristic value. It can also be observed, that a is again constant at 185 °C, thus showing that a linear increasing in the distribution function is within the range 160–185 °C.

Fig. 5b is a plot of b parameter against temperature. It can be seen that this parameter, that marks the symmetry for the times distribution, increases linearly with temperature and becomes stabilised at 185 °C, same as the parameter a. This means that the symmetry of the relaxation time distribution function increases with temperature, thus making the mean and the maximum values of this function to come close. This can be understood assuming the existence of a dipole with a dominant relaxation time. Values of the parameter b are in the range 0.6–0.75. Plots of ε_u versus temperature are shown in Fig. 5c. As can be seen, the unrelaxed permittivity increases linearly with temperature. This is because an increase in thermal mobility helps the different polarization processes apart of dipole contribution. This fact must be taken into account to modelize the behaviour of the system in a temperature study. This means that to model ε' and ε'' as functions of temperature (and not only on frequencies) ε_u is not a constant but a linear temperature function. ε_u values are lower than expected, could be due to a dielectric effect caused by an air gap between the electrodes and the resin. However, samples were as smooth as possible and were subjected to a considerable stress with the object of achieving a good contact between electrodes and sample, thus minimize the possible gap.

Fig. 5d is a $\varepsilon_r - T$ plot. It shows a practically linear increase of the relaxed permittivity with temperature, with a slope greater than that corresponding to the $\varepsilon_u - T$ plot. This is in contradiction with the behaviour expected through Onsager [23] equation that postulated ε_r be proportional to $1/T$. However, the Onsager expression has been used with moderate success to calculate dipole moments of simple polar molecules. In our case, ε_r is increased by increasing temperature, indicating that the dependence is mainly conducted by changes in the intramolecular interactions as is more generally the case of polymers.

As the slope of the linear plot shown in Fig. 5d is greater

Table 1
Parameters obtained from Havriliak–Negami fitting of ε' and ε'' versus f plots

T (K)	a	b	ε_u	ε_r	$\Delta\varepsilon$	τ (s)	σ (mho/cm)
433.15	4.1×10^{-4}	0.60946	2.287	3.712	1.425	1.73729	9.0797×10^{-15}
438.15	0.00909	0.60827	2.312	3.81	1.498	1.13405	9.1311×10^{-15}
443.15	–	0.63	2.309	3.86	1.551	0.67671	9.0447×10^{-15}
448.15	0.07738	0.66768	2.353	3.974	1.621	0.44749	9.1418×10^{-15}
453.15	0.09368	0.69261	2.362	3.986	1.624	0.27256	9.6771×10^{-15}
458.15	0.14255	0.76801	2.394	4.079	1.685	0.15236	8.5401×10^{-15}
463.15	0.14543	0.77966	2.452	4.17	1.718	0.08779	8.9636×10^{-15}
468.15	0.12993	0.77631	2.476	4.208	1.732	0.04742	9.2775×10^{-15}

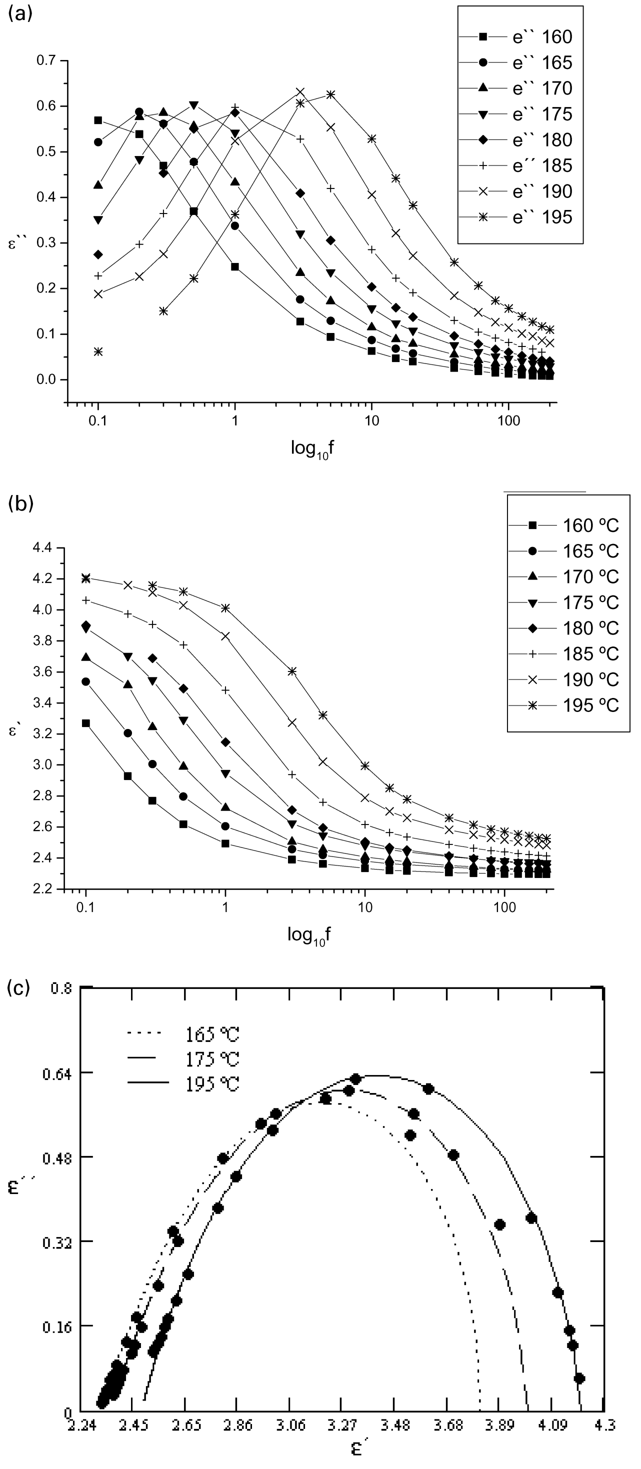

Fig. 4. (a) Dielectric dispersion curve (ε' vs. $^{10}\log f$) for the epoxy system DGEBA ($n = 0$)/1,2 DCH in the temperature range 160–195 °C. (b) Dielectric dispersion curve (ε'' vs. $^{10}\log f$) for the epoxy system DGEBA ($n = 0$)/1,2 DCH in the temperature range 160–195 °C. (c) Argand plot (ε' vs. ε'') for the epoxy system DGEBA ($n = 0$)/1,2 DCH at various temperatures in the range 160–195 °C.

than that corresponding to the plot shown in Fig. 5c, the difference $\Delta\varepsilon = \varepsilon_r - \varepsilon_u$ increases with temperature (see Fig. 5e). However, in studies made in our laboratories on the epoxy system *m*-xylylenediamine/DGBA($n = 0$) we found that ($\varepsilon_r - \varepsilon_u$) for the cured system diminishes with increasing temperatures. This means that this particular system changes polarizability with increasing temperature, that hides the decrease of $\Delta\varepsilon$ with temperature.

The different behaviour of these two epoxy systems could be understood on the basis of the stronger intersegmental interactions in the case of the DEGBA/1,2 DCH system.

The effect of diffusion on the kinetic study of both DEGBA/1,2 DCH and DEGBA/m-XDA has been previously studied [24,25] and shows different behaviour for free volume related parameters.

Both the relaxation time distribution width and its asymmetry are represented by the parameters here studied and they can be observed as a function of the temperature in the Argand diagrams shown in Fig. 4c. These diagrams were fitted using these parameters and Eq. (3). This figure shows that the system behaviour corresponds to a system showing neither conductivity nor an increase in ε'' at low frequencies.

3.1. Determination of the activation energy

The last parameter available from Havriliak–Negami equation is the characteristic relaxation time. Owing to its asymmetric distribution [26], this characteristic time results different from that obtained from the reciprocal of the frequency at which a maximum in the ε'' vs. f plot takes place.

Usually, this relaxation time is less than the characteristic relaxation time obtained as a parameter using the H–N expression.

Using the relationship $f = (2\pi\tau)^{-1}$, a frequency value can be assigned to each characteristic relaxation time and thus an Arrhenius plot as a function of temperature can be constructed. One other plot to be constructed is that representing the frequency of the different maxima vs. temperature.

Moreover, there is another relationship between frequency and temperature deriving from the T_g value associated to each frequency in the isochrone measurements.

Fig. 6 shows Arrhenius plots corresponding to the 3 kinds of data (Table 2). It can be seen that, at a given temperature, the value of the frequency obtained from the maximum in the range of frequencies is greater than that associated to the characteristic relaxation time, that in turns is greater than that associated to the isochrone measurements through T_g.

All the three plots show a linear behaviour with regression coefficients close to 0.997. This is mainly due to the narrow frequency range used for this study, that was imposed by the material degradation at temperatures around 280 °C.

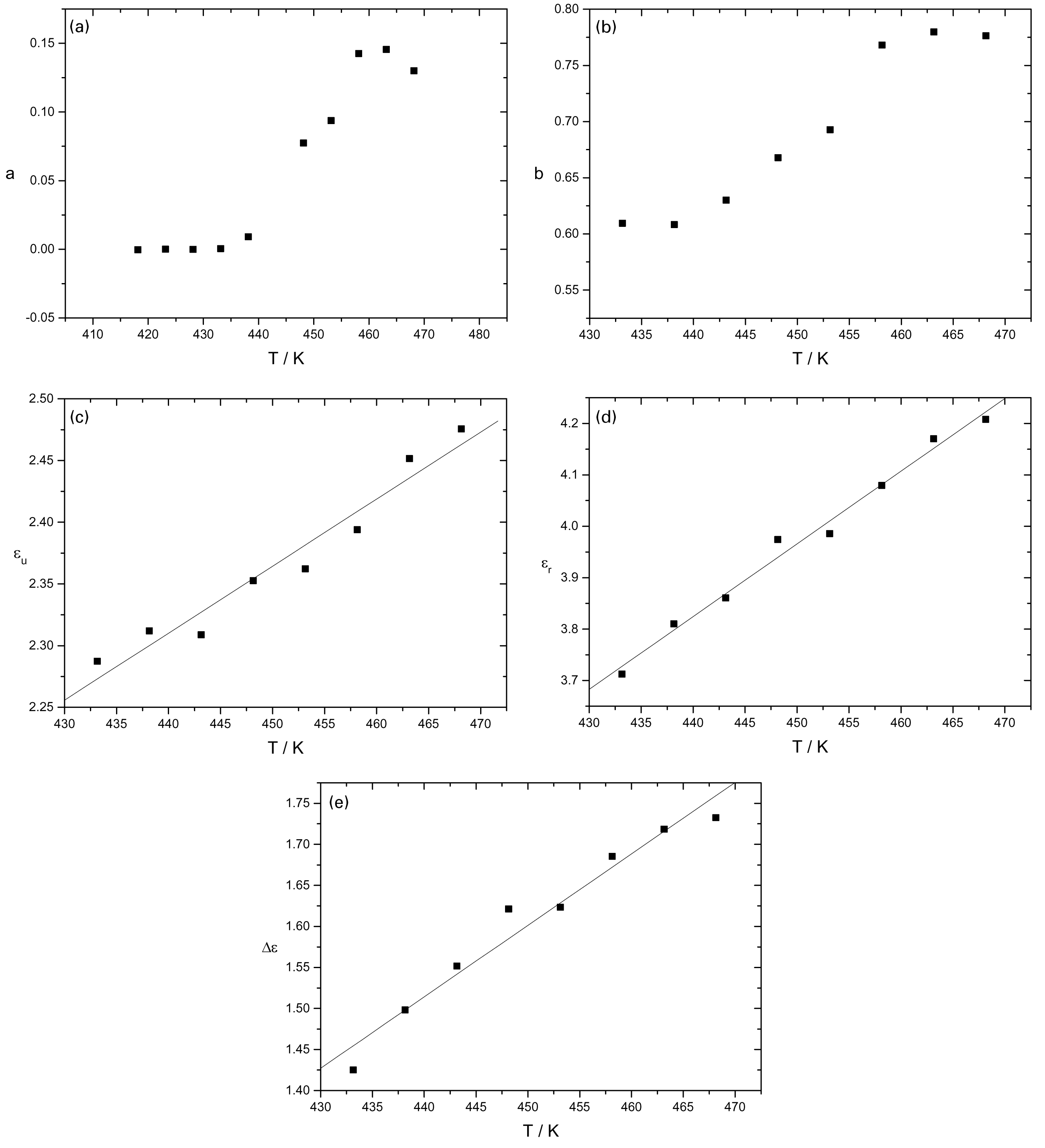

Fig. 5. (a) Plot of the parameter a (in H–N equation) versus temperature. (b) Plot of parameter b (in H–N equation) versus temperature. (c) Plot of unrelaxed permittivity versus temperature in the range from 160 to 195 °C. (d) Plot of the relaxed permitivity versus temperature in the range from 160 to 195 °C (DGEBA ($n = 0$)/1, 2 DCH). (e) Plot of $\Delta\varepsilon = \varepsilon_r - \varepsilon_u$ versus temperature in the range from 160 to 195 °C for the epoxy system DGEBA ($n = 0$)/1, 2 DCH.

For this reason, it is possible to use the Arrhenius model for data fitting.

$$f = f_0\, e^{-\frac{E_a}{RT}} \qquad (6)$$

where f is the constant frequency corresponding to each experiment, f_0 is a constant value, R is the gas constant, T is the adequate temperature in any of the three cases, commonly associated to T_g, and E_a is the activation energy.

Different values for the activation energy were determined depending on the method used: 180.1 kJ mol^{-1} from ε'' maximum within the range of frequencies, 167.8 kJ mol^{-1} from data supplied by the characteristic relaxation time in H–N equation, and

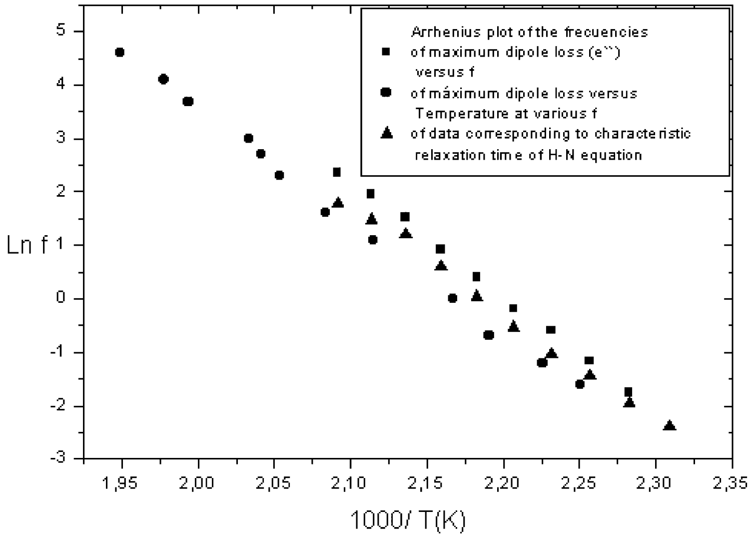

Fig. 6. Arrhenius plot of the alpha transition of the epoxy system DGEBA ($n = 0$)/1, 2 DCH.

176.3 kJ mol^{-1} from values of the maximum within the temperature range.

It can be seen that the E_a values obtained using ε'' maxima, both in temperature or frequency range, are very similar and slightly greater than those obtained from the characteristic relaxation time.

Even if the difference is relatively small, it must be taken into account.

An Arrhenius plot of σ vs. T was constructed to study more accurately the quantitative difference between the dipole relaxation and conductivity processes (Fig. 7).

Values of σ, at each temperature, were calculated by fitting data of ε'' vs. ω in the zone of low frequencies until the frequency values at which an important increase in ε'' was detected, thus indicating that the process is governed by conductivity.

Table 2
Data used for construction of the three Arrhenius plots shown in Fig. 6

[a]*T* (K)	[a]*f* (Hz)	[b]*T* (K)	[b]*f* (Hz)	[c]*T* (K)	[c]*f* (Hz)
444.29	0.2	433.15	0.5756	438.15	1.08667
449.27	0.3	438.15	0.88197	443.15	1.96424
456.44	0.5	443.15	1.47768	448.15	3.48852
461.5	1	448.15	2.23487	453.15	5.23155
472.85	3	453.15	3.66875	458.15	9.39011
479.89	5	458.15	6.56367	463.15	15.83364
486.96	10	463.15	11.39072	468.15	29.15385
489.76	15	468.15	21.08744	473.15	44.73191
491.76	20	473.15	27.45061	478.15	65.91111
501.58	40	478.15	37.51407		
505.66	60				
513.03	100				

[a] Temperature corresponding to ε'' maximum in $\varepsilon'' - T$ plots at the different measurement frequencies.

[b] Frequencies obtained from the reciprocal of relaxation time using H–N equation at different temperatures.

[c] Frequencies corresponding to ε'' maximum in $\varepsilon'' - f$ plots at the different isothermal measurements temperatures.

A linear behaviour was observed, thus allowing the use of the Arrhenius equation for determination of the activation energy. This Arrhenius value results 373.5 kJ mol^{-1}, that is 2.1 times greater than the value obtained for the dipole relaxation. This indicates that to initiate the conductivity processes requires a greater energy than that necessary to start the dipole relaxation.

This apparently great value of the activation energy might be due to the high crosslinking density because of the short distance between active centres. This high crosslinking density is directly related to the great T_g of this system [27].

4. Conclusions

Dielectric analysis was used to study the glass transition of a cured epoxy system Diglycidyl ether of bisphenol A/1,2 diaminecyclohexane.

Experimental data were analysed using the Havriliak–Negami equation. This analysis shows that the α-relaxation is characterized by an increase in the relaxation time distribution width and also that this distribution becomes asymmetrical with temperature decrease. The increase in the distribution width starts from 160 °C, 15 °C above the glass transition temperature measured by DSC. Below this temperature the parameter a of the H–N equation is practically zero.

This result, joined to the fact that $\Delta\varepsilon$ increases linearly with temperature, suggest an increase in the number of dipoles contributing to an increase in permittivity and also that these dipoles present different configurations as can be deducted from the study of the parameters a and b.

It can be also observed that ionic conductivity is only significant at temperatures well above the temperature range used in this study. This also demonstrates that, for cured thermosets, the processes controlling the dipole relaxation

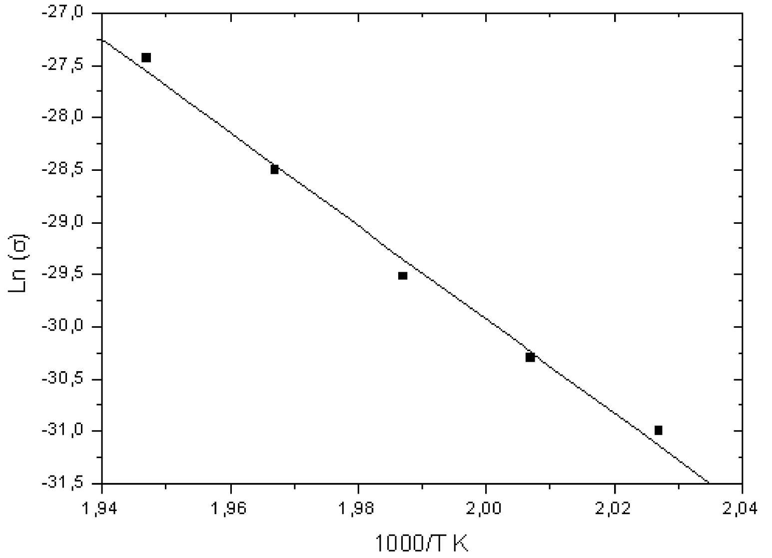

Fig. 7. Arrhenius plot of the conductivity for the epoxy system DGEBA ($n = 0$)/1, 2 DCH.

and the ionic conductivity are different from the qualitative point of view.

Within the temperature and frequency ranges studied, both frequency and temperature follow an Arrhenius-like behaviour.

A quantitative difference was observed, depending on the election of the reciprocal of the time corresponding to the maxima in ε'' vs. f plots, or the characteristic relaxation time obtained using H–N equation. The asymmetry observed in the relaxation time distribution goes in the sense that τ maximum is lower than the characteristic relaxation time. The values obtained for the activation energy are close to 178 kJ mol^{-1}.

It was also observed that, within the frequency and temperature ranges used for this study, the conductivity follows an Arrhenius-like behaviour. However, the associated activation energy was found to be 373 kJ mol^{-1}, very much greater than that found for the dipole relaxation.

References

[1] Abuín S, Pazos M, Núñez L. J Appl Polym Sci 1990;41:2155.
[2] Abuín S, Pazos M, Núñez L, Simal J, Paseiro P. J Appl Polym Sci 1993;47:533.
[3] Pazos Pellín M, Núñez Regueira L, López Quintela A, Paseiro Losada P, Simal Gándara J, Paz Abuín S. J Appl Polym Sci 1995;55:1507.
[4] Núñez L, Fraga F, Castro A, Fraga LJ. Thermal Anal 1998;52:1013.
[5] Núñez L, Fraga F, Núñez MR, Castro A, Fraga L. J Appl Polym Sci 1999;74:2997.
[6] Brown ME. Principles and practice. Handbook of thermal analysis and calorimetry, Vol. 1. Amsterdam: Elsevier; 1998.
[7] McCrum NG, Read ME, Williams G. Anelastic and dielectric effects in polymeric solids. New York: Wiley; 1967.
[8] Coln MCW, Senturia SD. The application of linear system theory to parametric microsensor. Proc Transducers'85 1985;118.
[9] Turi EA. Thermal characterization of polymeric materials. San Diego: Academic Press; 1997. p. 1518–1523.
[10] Hunt BJ, James MI. Polymer characterisation. Great Britain: Blackie Academic and Professional; 1993.
[11] Sheppard Jr. NF, Senturia SD. J Polym Sci: Part B: Polym Phys 1989; 27:753.
[12] Senturia SD, Sheppard Jr.NF. Dielectric analysis of thermoset cure. Advances in polymer science, vol. 80. Berlin: Springer; 1986.
[13] Debye P. Polar molecules. New York: Chemical Catalog Co; 1929.
[14] Cole KS, Cole RH. J Chem Phys 1941;9:341.
[15] Davidson DW, Cole RH. J Phys Chem 1951;19(12):1484.
[16] Havriliak S, Negami S. Polym Sci C 1966;14:99.
[17] Havriliak S, Negami S. Polymer 1967;8:161.
[18] Núñez L, Fraga F, Núñez MR, Villanueva M. J Appl Polym Sci 1998; 70:1931.
[19] Meseguer Dueñas JM, Torres Escuriola D, Gallego Ferrer G, Monleón Pradas M, Gómez Ribelles JL, Pissis P, Kyritsis A. Macromolecules 2001;34:5525.
[20] Bisdrup SA, Day DR. Assignment of the glass transition. Seyler RJ, editor. Am Soc Test Mater, Philadelphia 1994;108–19.
[21] Day DR, Lewis TJ, Lee HL, Senturia SD. J Adhes 1985;18:73.
[22] Havriliak S, Havriliak SJ. Dielectric and mechanical relaxation in materials (analysis, interpretation, and application to polymers). Cincinnati: Hanser/Gardner Publicationes; 1997.
[23] Böttcher CJF, Bordewijk P. Theory of polarization. Dielectrics in time-dependent fields, vol. II. Amsterdam: Elsevier; 1978.
[24] Núñez L, Fraga F, Núñez MR, Villanueva M. J Appl Polym Sci 1998; 70:1938.
[25] Núñez L, Fraga F, Núñez MR, Castro A, Fraga L. J Appl Polym Sci 1999;74:2997.
[26] Williams ML, Landel RF, Ferry JD. J Am Chem Soc 1955;77:3701.
[27] Lopez-Quintela A, Prendes P, Pazos-Pellin M, Paz M, Paz-Abuin S. Macromolecules 1998;31:4770.